

Fuzzy-Based Classification of Breast Lesions Using Ultrasound Echography and Elastography

Shirley Selvan, ME,* M. Kavitha, ME,* S. Shenbaga Devi, ME, PhD,* and S. Suresh, MBBS, FRCOG†

Abstract: Common breast lesions have different elasticity properties. Segmentation of contours of breast lesions from elastography and B mode images by incorporating variational level set method is involved in the proposed work. After segmentation, strain and shape features, such as differences in area, perimeter, and contour and width to height difference and solidity, as well as texture features like contrast, entropy, standard deviation, dissimilarity, homogeneity and energy, are estimated. A nonlinear fuzzy inference system is applied for classifying the breast lesions as benign cyst, benign solid mass, or malignant solid mass. Detection of malignant solid masses is our primary objective. A classification accuracy of 83% is obtained. One hundred percent sensitivity is reported. It can be concluded that the proposed fuzzy-based classification technique can be used as an aid for the automated detection of breast lesions.

Key Words: fuzzy, elastography, characterization, breast lesions

(*Ultrasound Quarterly* 2012;28:159–167)

The noninvasive methods used to diagnose breast cancer have limitations. Currently, detection techniques are based primarily on physical examination, mammography, sonography, and magnetic resonance imaging. The most sensitive non-invasive modality for detecting breast cancer is the magnetic resonance imaging. The ultrasound has long been used to distinguish between benign, fluid-filled cysts and solid masses. However, solid masses are often not malignant. For example, both fibroadenomas and scirrhous carcinomas are solid and stiff, but only the latter are malignant. Results show that, under small deformation conditions, the elastic modulus of normal breast fat and fibroglandular tissues are similar, whereas fibroadenomas are of approximately twice the stiffness. A 3- to 6-fold increase in stiffness is exhibited by fibrocystic disease and malignant tumors. A 13-fold increase in stiffness is exhibited by high-grade invasive ductal carcinoma when compared with fibroglandular tissue.¹ The B-mode sonographic features for benign and malignant lesions have been shown to overlap each other substantially.²

Imaging of dense breast tissue in mammography³ is also difficult. These limitations of mammography and sonography

and the need, not to miss a malignant lesion in the early stage of disease have lead to invasive surgical biopsy causing patient discomfort, anxiety and hospitalization in addition to increasing costs to the patient. This substantial problem in breast cancer diagnosis remains. Elastography increases the specificity in diagnosis and reduces the chance of interventional procedure for a biopsy and should reduce patient discomfort associated with mammography.

Elastography is a technique capable of producing images of internal strain or young's modulus of soft tissues. It involves steps of obtaining ultrasonic scan of the target, subjecting the target to a small mechanical compression and obtaining a second scan of the same region. Radiofrequency waveforms of the 2 scans received from a small segment of tissue at a given depth are cross correlated to find the time delay between the 2 waveforms. The time delay is related to mechanical displacement of the tissue at a given depth. The rate of change in tissue displacement as a function of depth is known as strain. If the applied axial stresses are known or assumed constant in the target, the strain values are directly converted to elastic modulus values. The gray levels on the resulting image will ultimately correspond to tissue elasticity. This image is called an elastogram.⁴

Mechanical measurements have shown that pathological tissue can be up to 30 times stiffer than normal tissue.⁵ Ultrasound elastography is described as the method for measuring the stiffness/elastic properties of tissues^{2,6–8} by Ophir et al.^{4,9,10} The comparison of spatial arrangement of tissue before and after compression is the basic operating principle of elastography. This scanning modality, which can provide information about stiffness of lesions, is being used for detecting and identifying lesions in the breast currently. Paired images, consisting of the standard B-mode image on the left and a pure strain image on the right,¹¹ are obtained.

Benign lesions usually appear smaller or of the same size on sonograms as well as on elastograms. In case of malignant lesions, the size seems larger on the elastogram.^{12,13} Benign lesions tend to have smoother borders and are loosely bound to adjacent tissue and are more mobile. Most malignant tumors tend to form speculated margins, although some types of malignant tumors could have smooth margins. It has therefore been observed that during an applied compression, benign lesions tend to undergo motion in an opposite direction to that of the compression.¹⁴ On the other hand, malignant lesions move in the direction of compression while pulling the perilesional tissue in the same direction, thereby causing the perilesional tissue also to appear stiffer on the elastogram as well. Studies have demonstrated that B-scan ultrasound imaging tends to underestimate the size of a tumor compared with

Received for publication August 15, 2011; accepted March 19, 2012.

*Department of Medical Electronics, College of Engineering, Anna University; and †Mediscan Systems, Foetal Care Research Centre, Chennai, Tamil Nadu, India.

The authors declare no conflict of interest.

Reprints: Shirley Selvan, Anna University, No 39 a, First Main Rd, Aps Colony, Velachery, Chennai, India 600042 (e-mail: shirleycharlethentry@gmail.com).

Copyright © 2012 by Lippincott Williams & Wilkins

pathology measurement. The size of a breast tumor is larger in elasticity images than in B-scan ultrasound images, and it is a reasonable hypothesis that the tumor size in elasticity images is a more accurate representation than that measured at pathology.¹⁰

The breast is an ideal organ on which to perform elastography because of the ease with which it can be compressed. Elastography, which estimates tissue stiffness, may be an attractive tool for distinguishing benign from malignant lesions because of the relative stiffness of breast cancer tissue as compared with benign fibroadenomas and cysts.

In the diagnosis of breast cancer using elastography, several diagnostic criteria, such as lesion visualization, relative brightness, and margin irregularity by capturing the radio-frequency data of the reflected echoes after giving compression to the lesion, have been proposed by Garra et al¹⁵ and Hall et al.¹¹ Instead of radiofrequency data, continuous ultrasound images obtained through probe compression were used by Steinberg et al¹⁶ and Moon and Chang.¹⁷

Automated detection of tumor margin in breast elastography is desired for diagnostic purposes. A preliminary segmentation algorithm using the coarse-to-fine active contour method was proposed by Wu Liu et al.¹⁸ This method is effective for segmenting regions of images that have a relatively regular, well-circumscribed single margin but might not be effective in segmenting spiculated masses with irregular margins as seen in malignant tissue.

Xia's method¹⁹ refers to contour evolution, which improves on the coarse-to-fine active contour method proposed by Liu et al.¹⁸ This method can handle features that the active contour method has difficulties with, including self intersecting contours and changes in topology.

In this work, a fully automated fuzzy-based classifier to diagnose breast lesions is proposed. Ultrasound and elastography image pair of a breast lesion is acquired. The contours of a breast lesion are evolved from the acquired image pair. The lesion areas in ultrasound and elastography images are segmented. Three sets of features, namely texture, strain, and shape, are computed from the segmented lesion areas in ultrasound and elastography images. A total of 17 features are extracted from each image pair. Based on Student *t* test, 5 statistically significant features are selected. A fuzzy logic system has been designed with these 5 features and a set of rules. The fuzzy logic system is evaluated for the test images. This proposed system is used to detect the type of lesion, namely, benign cyst, benign solid mass, and malignant solid mass.

METHODOLOGY

Image Acquisition

This study is a retrospective analysis of stored images and has no impact on the clinical management of the patients, as all the patients have already been treated or undergone treatment. The stored images used for the study were anonymous. The ultrasound and elastography images of 40 biopsy proven lesions were taken from the database. All images were obtained on a Siemens ACUSON Antares scanner with a high-frequency linear VF 7-3 MHz transducer from July 2007 to March 2009.

Segmenting the Lesion

Because of noise and speckles in the ultrasound B-scan and elastographic images, noise filtering and edge enhancement are required. The image quality is significantly improved by the SRAD filter²⁰ while preserving the important boundary information, and hence, in the present study, speckle-reducing anisotropic diffusion filtering of real elastography and ultrasound B-scan images is done to reduce noise and speckles.

Segmentation is required to separate the tumor region from its background. Segmentation algorithms for gray scale images are based on one of the 2 basic properties of image intensity values: discontinuity and similarity. In the first category, the image is partitioned based on abrupt changes in the intensity, such as edges in an image. In the second category, the image is partitioned into 2 regions that are similar according to a set of predefined criteria.

In the present study, the "level set active contour method"²¹ based on the second criteria is used for segmentation. Here, the initial contours of lesions of both ultrasound and elastography images are determined by the method proposed by Xia et al.¹⁹ In this method, shape and region information are incorporated into the level set energy functions. It is more robust than the method originally proposed by Osher and Sethian.²²

The following steps are involved in the automatic lesion segmentation algorithm: (1) preprocessing of elastography and ultrasound B scan images by SRAD filter¹⁶ to reduce noise and speckles, (2) gray value thresholding²³ of the pre-processed image to obtain a binary image, (3) selecting a binary mask from the image, and (5) applying level set algorithm to segment the area of lesion. This algorithm has been applied to both ultrasound B-scan and elastography images. The segmentation results are shown in Figures 1 to 4. The various stages of filtering and segmentation of US B-scan images and elastograms of a malignant solid mass, benign solid mass, and benign cysts are also shown in Figures 1 to 4. The computed delineated margin is the white outline. Malignant masses are stiffer and, therefore, deform less than benign masses. They appear darker and larger than benign masses on an elastogram. A benign lesion can appear significantly smaller on an elastogram.¹³ A cyst is characterized by its inner anechoic substance and thin echogenic outer wall. It is depicted as nidus (bull's eye appearance) in an elastogram (Fig. 4C). The bull's eye artifact has a posterior bright spot in addition to the central white spot. Lesions other than cysts can have only the central white spot.²⁴

Feature Extraction

The automatic feature extraction methodology from breast ultrasound and elastography images used in this work has been described extensively elsewhere²⁵ and will only be briefly summarized here.

Based on the difference in size and shape of malignant, benign and cystic lesions in elasticity images and B-scan ultrasound images,^{10,12,26} 5 features were extracted for each computer-determined lesion contour: area difference, perimeter difference, contour difference, solidity, and width-to-height ratio.²⁷ Based on the fact that texture features represent changes of gray level intensity, 6 second-order statistical features were

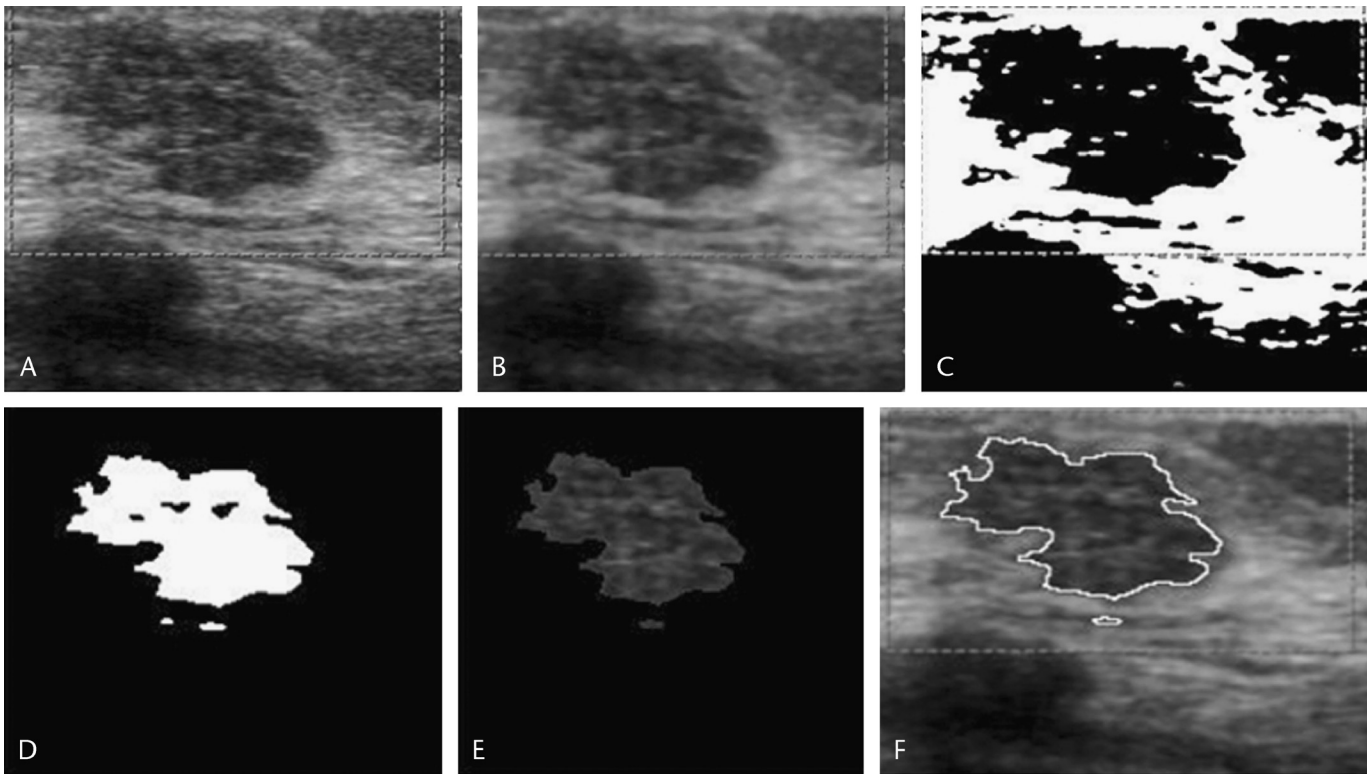


FIGURE 1. A, Original ultrasound B mode image of malignant solid mass. B, Filtered image. C, Image after applying automatic threshold Figure 1D. Final contour. E, Segmented tumor (ROI). F, Computer delineated margin of malignant solid mass in an ultrasound B mode image.

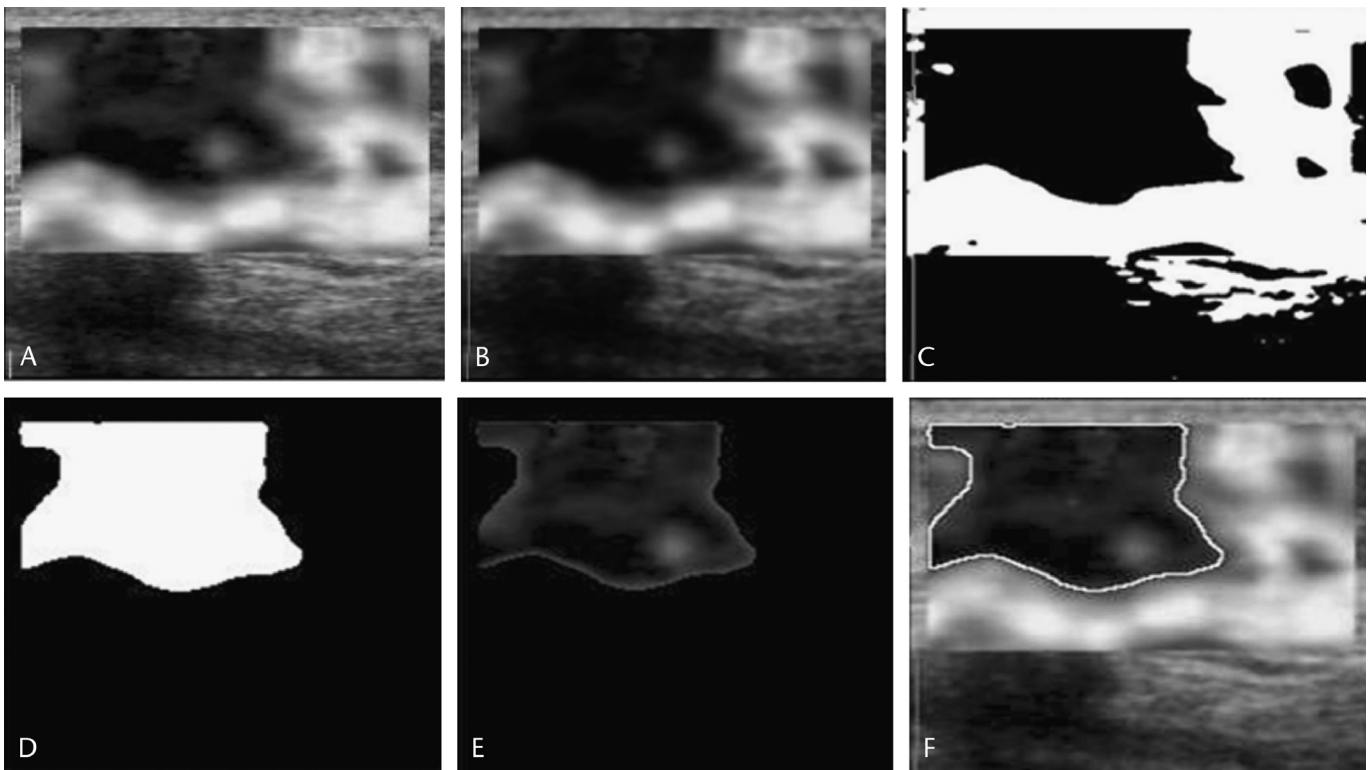


FIGURE 2. A, Original elastogram of malignant solid mass. B, Filtered image. C, Image after applying automatic threshold. D, Final contour. E, Segmented tumor (ROI). F, Computer delineated margin of malignant solid mass in an elastogram.

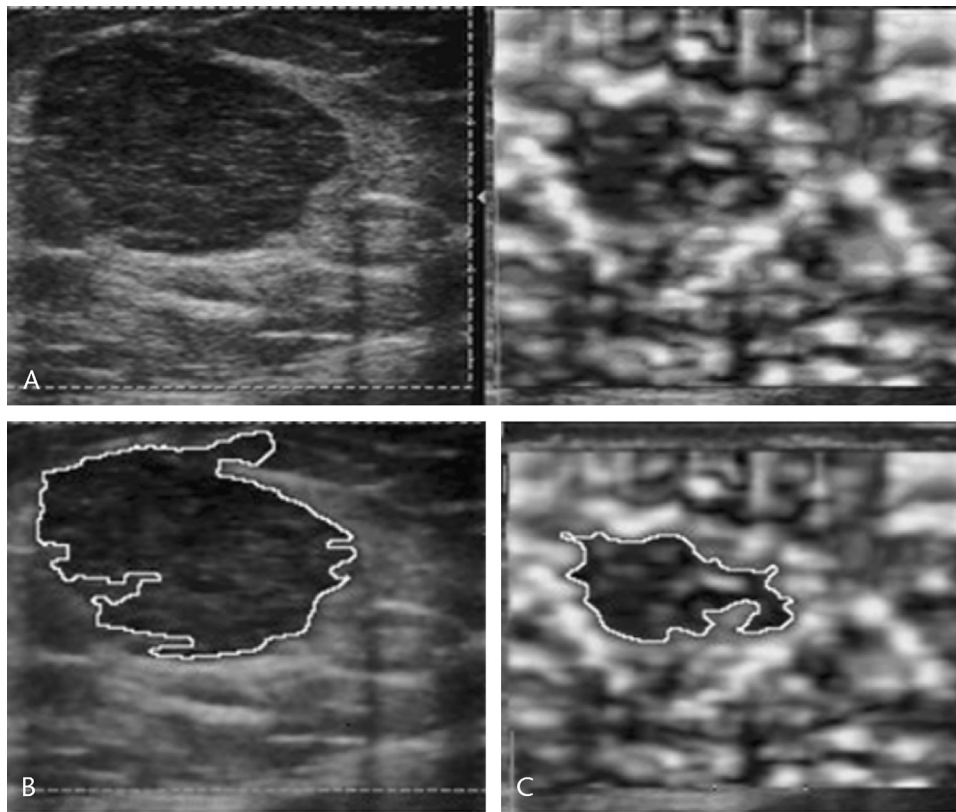


FIGURE 3. A, Ultrasound image and elastogram of a benign solid mass. B, Computer delineated margin of benign solid mass in ultrasound image. C, Computer delineated margin of benign solid mass in an elastogram.

computed for each computer-determined lesion contour from the gray level co-occurrence matrix²⁸: standard deviation, energy, entropy, dissimilarity, homogeneity, and contrast.

The classification stage of the system, which uses these features, is described in the following subsection.

Classifier

In this work, an approach based on fuzzy logic system (FLS)²⁹ has been used to classify the types of lesions. The schematic of the proposed fuzzy based classifier is shown in Figure 5. A fuzzy logic system (FLS) is an expert system, which is computer based and that which emulates the reasoning process of a human expert within a specific domain of knowledge. A FLS consists of 4 main modules: fuzzification module, fuzzy rule base, fuzzy inference engine, and defuzzification module. Our proposed FLS used for classification of breast lesions using ultrasound echography and elastography consists of 5 inputs, namely, area difference, solidity, perimeter difference, energy and contrast, and one output namely type of lesion. The schematic of the proposed FLS is shown in Figure 6. The main issues involved in the system design are as follows:

- A crisp set of the input and output variables and their range of values are considered. For example, the range of input linguistic variable solidity is between 0.2 and 0.8.
- A crisp set of the input and output variables are expressed as fuzzy sets using linguistic variables, linguistic states, and membership functions. This step is fuzzification. For

example, solidity is an input linguistic variable, which describes regularity of the lesion. Solidity is represented by 4 linguistic states or 4 degrees of membership, namely, lower, low, high, and higher. Each linguistic state is represented by a Gaussian membership function. Likewise, the other input variables are fuzzy quantized. The output variable, namely, type of lesion, is represented by 3 linguistic states or 3 degrees of membership, namely, benign solid mass, malignant solid mass, and benign cyst. These states are represented by fuzzy sets with triangular membership function.

- The rules are constructed based on the description of the input and output variables. The rules are stored in the fuzzy rule base. For example, the variable area difference is used to compare areas of lesions between 2 images (ultrasound image and elastogram), as lesion area changes in accordance to the applied pressure. The area difference is defined as the difference between areas of lesions in the ultrasound images and elastograms.

The feature solidity is used to describe the regularity or shape of lesions. Benign solid mass usually have smooth shapes, so they produce a regular shape in both ultrasound and elastography images, whereas malignant solid mass present irregular shapes in elastograms because of their solid nature. Based on the description of area difference and solidity, the rule reads: if area difference is highly negative or solidity is lower, then type of lesion is malignant. Likewise, the other 4 rules are written.

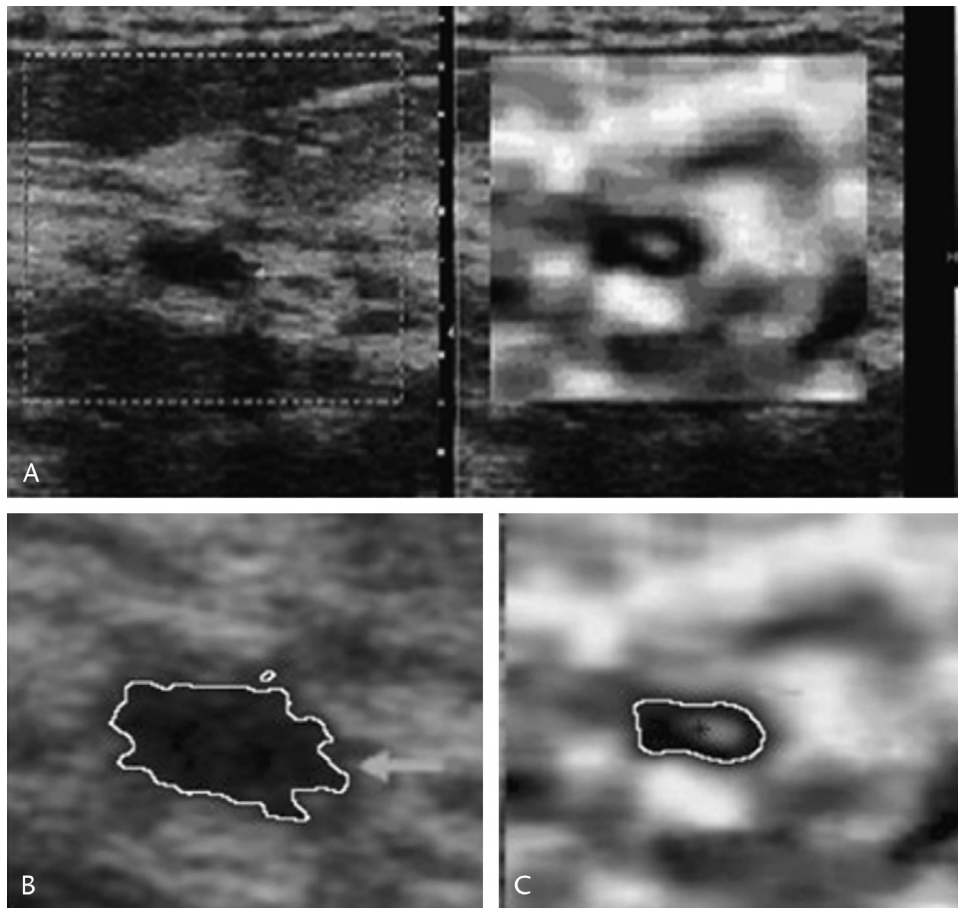


FIGURE 4. A, Ultrasound image and elastogram of a cystic lesion. B, Computer delineated margin of a cyst in an ultrasound image. C, Computer delineated margin of a cyst in an elastogram.

- The fuzzified measurements are used by the inference engine to evaluate the set of rules. The membership functions on the input variable, for example, solidity are applied to

their actual values to determine the degree of truth for rule premise. This degree is referred to as its alpha value. The alpha value of each rule is applied to the consequent of that

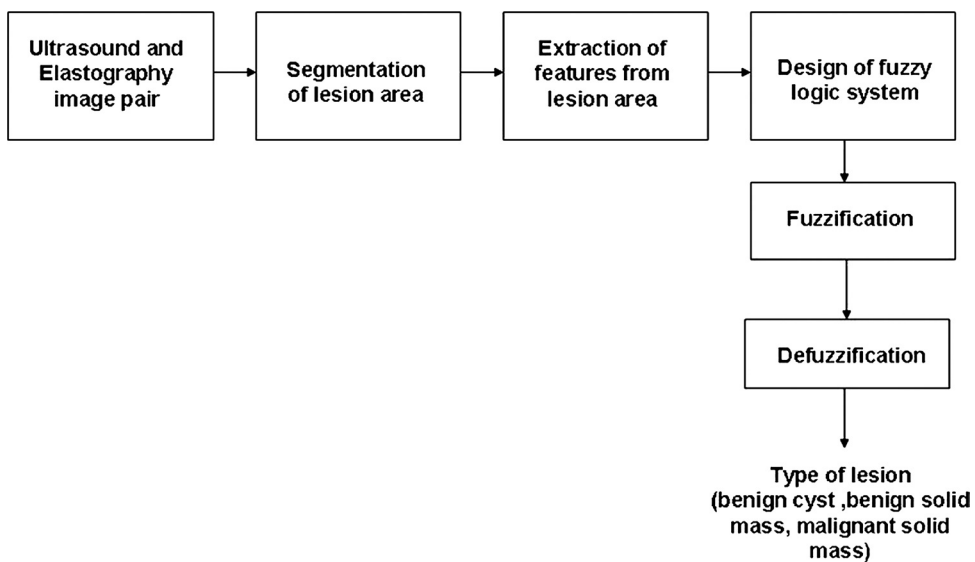


FIGURE 5. Fuzzy-based classifier of breast lesions.

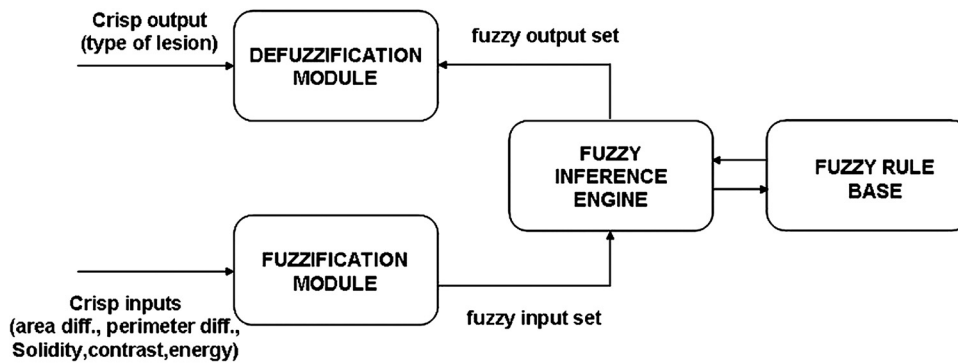


FIGURE 6. Fuzzy logic system.

rule. This results in one fuzzy set being assigned to output variable of each rule. The various output fuzzy sets are aggregated into a single fuzzy set. This step is called inference.

- The aggregate of a fuzzy set resulting from inference encompasses a range of output values and is defuzzified to obtain a final crisp output. This step is defuzzification. The crisp output is the type of lesion (benign cyst, benign solid mass, and malignant solid mass).

The fuzzy inference engine used in the proposed FLS is shown in Figure 7. Tumor areas between ultrasound B mode and elastography images are compared using area difference, as tumor area changes according to the pressure exerted.¹⁷ Area difference is less for a malignant solid mass and high for benign solid mass. The input variable area difference has 4 degrees of membership, namely, high positive, positive, negative, and high negative. Regularity of a lesion is represented using solidity. Malignant solid mass with spiculated margins have a low value of solidity and benign solid mass with smooth borders have high value of solidity. The input variable solidity has 4 degrees of membership, namely, high, higher, low, and lower. Perimeters of lesions in B-scan and strain images are compared using perimeter difference. Perimeter refers to the number of pixels in the boundary of lesions. Perimeter difference is high for both benign lesions and cysts. Energy is a measure of uniformity of intensity distribution or orderliness in the lesion area. Contrast refers to local intensity variations in the lesion area. Energy and contrast are higher for a benign lesion when compared with a cyst. The input variables perimeter difference, energy, and contrast have 2 degrees of membership, namely, low and high. The degrees of membership of the input variables are shown in Table 4. The fuzzy rule base accommodates 5 rules. The output variable “type of lesion” has 3 degrees of membership, namely, benign solid mass, malignant solid mass, and benign cyst.

Rules

- If area difference is highly negative or solidity is lower, then type of lesion is malignant solid mass.
- If area difference is highly positive or solidity is higher and, contrast and energy are high, then the lesion is a benign cyst.
- If area difference, solidity, perimeter difference, energy, and contrast are high, then the lesion is a benign cyst.

- If area difference is highly positive or solidity is higher and contrast and energy are low, then the lesion is benign solid mass.
- If the area difference, solidity, and perimeter difference are high and energy and contrast are low, then the lesion is benign solid mass.

Once the classifier is designed, it is evaluated using jack-knife procedure. Fifty percent of the training set is used for training, and the rest is used for testing such that there is no overlap between data. The classification of lesion is done after evaluating the classifier for the test images.

RESULTS AND DISCUSSION

This study is applicable to strain images. These images have stiff areas, which seem black, whereas less stiff tissue seems white. The above algorithm has been tested on 40 pairs of ultrasound and elastogram biopsy-proven images wherein 11 are benign cyst, 16 are benign solid mass and

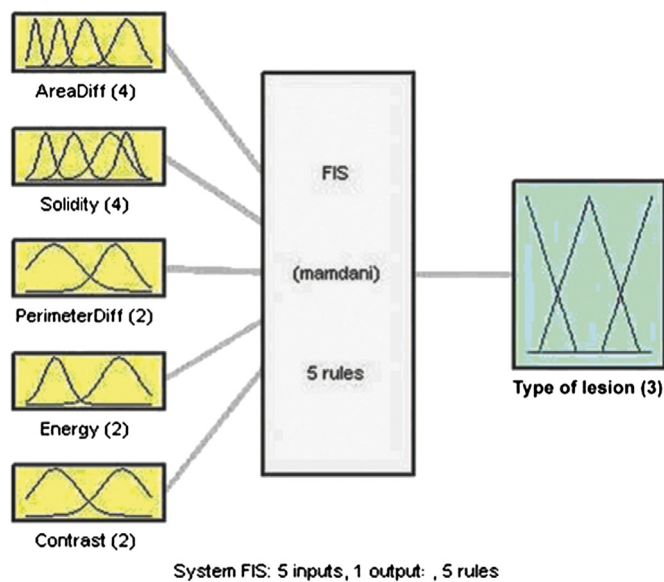


FIGURE 7. Fuzzy inference engine.

TABLE 1. Texture Features of Ultrasound Image Showing Range of Values

Features	Benign Solid Mass	Malignant Solid Mass	Benign Cyst
Energy	10,000–50,000	500–10,000	7000–43,000
Entropy	–830 to –1290	–120 to –280	–2000 to –16,000
Dissimilarity	100–500	40–10,000	3000–15,000
Homogeneity	30–430	57–78	300–2000
Contrast	100 to 1000	150–3000	450–20,000
SD	20–60	0.22–1.0	0.6–35

13 malignant solid mass. The gold standard here is that all the images are biopsy proven.

Segmentation

The segmentation results are shown in Figures 1 to 4. Figures 1A to F show the various stages of filtering and segmentation of a US B-scan image of a malignant solid mass. Figures 2A–F show the various stages of filtering and segmentation of an elastogram of a malignant solid mass. Figures 3A–C show the ultrasound image and elastogram of a benign solid mass and their segmented images. Figures 4A–C show the ultrasound image and elastogram of a cystic solid mass and their segmented images. The computed delineated margin is the white outline shown in Figures 1F, 2F, 3B, 3C; 4B, and 4C.

Feature Extraction

The features extracted are listed in Tables 1 to 3. Table 1 presents the texture features of malignant solid masses, benign solid masses and benign cysts of a US B-scan image. Table 2 presents the texture features of malignant solid masses, benign solid masses and benign cysts of an elastogram. Table 3 presents the strain and shape features obtained from parameters of both US B-scan and elastography images.

Differences between the 6 values for elastogram and ultrasound B-scan texture features and 5 strain/shape features in benign, malignant and cystic lesions were evaluated using the Student *t* test. For each analysis, a *P* < 0.05 was considered to indicate a significant difference.

When the difference between the elastogram entropy of a benign lesion and the elastogram entropy of a malignant lesion was used to compare groups, the entropies for the group with malignancy and that with benign nature were statistically significantly different (*P* = 0.0012). With use of the same parameter, the mean value of the benign group was not statistically significant from that of the group with cysts (*P* = 0.25567).

TABLE 2. Texture Features of Elastography Image Showing Range of Values

Features	Benign Solid Mass	Malignant Solid Mass	Benign Cyst
Energy	300–1000	2000–8000	3000–20,000
Entropy	–60 to –540	–300 to –500	–780 to –8000
Dissimilarity	3000–4000	80–1200	1300–20,000
Homogeneity	52–278	268–530	160–1000
Contrast	100 to 1000	90–2500	430–3000
SD	0.1–0.25	0.7–40	0.39–0.84

TABLE 3. Strain and Shape Features From Ultrasound and Elastography Images

Features	Benign Solid Mass and Benign Cyst	Malignant Solid Mass
Area difference	5–100	–60 to –10000
Solidity	0.6–0.8	0.2–0.6
Perimeter difference	10–100	100–1000
Contour difference	7–100	1–10
Width-height ratio	–40 to –150	15–100

The entropies for the malignant group and group with cysts were statistically significantly different (*P* = 0.022). Differences between benign and malignant breast tumors were statistically very significant for values of elastographic homogeneity (*P* = 0.0006). With use of the same parameter, the mean value of the benign group was not statistically significant from that of the group with cysts (*P* = 0.2839), although the mean values of the malignant group with benign group were close to being statistically significant (*P* = 0.0227). The difference between malignant and cyst were statistically very significant for values of elastographic dissimilarity (*P* = 0.005), although the mean values of the malignant group with cystic group were close to being statistically significant (*P* = 0.0244). The difference between benign solid mass and malignant solid mass, benign cyst and benign solid mass, malignant solid mass and benign cyst were not statistically significant for elastographic texture features energy, contrast, and SD.

The difference between benign and malignant, cyst and benign, malignant and cyst were not statistically significant for ultrasound B-scan texture features energy, entropy, homogeneity, and SD. The difference between malignant and cyst were statistically significant for values of sonogram dissimilarity (*P* = 0.05), and the difference between benign and cyst were statistically significant for values of sonogram contrast (*P* = 0.03).

The difference between malignant solid mass and benign cyst were statistically very significant for values of solidity, the

TABLE 4. Mean and Standard Deviation Values of FIS Inputs From 40 Image Pairs

Name of the Parameter	Membership Functions	Mean	Standard Deviation
Area Difference	High positive	57.77045	21.35105
	Positive	14.30632	8.04699
	Negative	–47.7126	16.82579
	High negative	–2501.58	4143.39
Solidity	High	0.621856	0.051623
	Higher	0.918981	0.07354
	Low	0.463416	0.027538
	Lower	0.179155	0.144788
Perimeter Difference	Low	–240.01	540.1314
	High	38.38749	31.74387
Energy	Low	5529.455	1301.083
	High	48685.88	66280.76
Contrast	Low	2097.333	912.7351
	High	8401.091	4928.523

TABLE 5. Correct Classification Rate of the FIS Classifier

Type of Lesion	Total Number	Correctly Detected	Correct Classification Rate (%)
Benign cyst	11	7	64
Benign solid mass	16	13	82
Malignant solid mass	13	13	100

shape feature. ($P = 0.004$). The difference between malignant and benign were statistically significant for values of solidity ($P = 0.016$) and width-to-height difference ($P = 0.023$). Hence, in conclusion, it is appropriate to combine the information obtained from both US elastography and US B-scan images for better diagnosis. The mean and SD values of membership functions are listed in Table 4.

Classification

Forty sets of ultrasound B-scan images and elastograms are used for testing, of which, 27 are benign (including 11 cysts and 16 benign solid masses) and 13 are malignant lesions. Of the 13 malignant lesions, 13 lesions are detected (TP), and none is not detected (FN). Of the 27 benign lesions, 20 are detected (TN), and 6 are misinterpreted as malignant (FP) and one cyst as benign. Table 5 lists the parameters of evaluation for the proposed algorithm.

The performance analysis is listed in Table 6. A classification accuracy of 83% is obtained. The sensitivity of classifier in detecting malignant solid mass is 100%, and specificity in detecting benign solid mass and benign cyst is 74%.

This algorithm works well for malignant solid mass but fails for simple cysts. Most elastographic cysts have an anechoic and thin echoic portion. However, in certain cases of cysts, it was possible to segment the anechoic portion only. Texture, strain, and shape features are extracted from this anechoic portion. However, these features were not representative of simple cysts, which led to wrong classification.

CONCLUSIONS

In this proposed method, the 2 sets of images are initially preprocessed by anisotropic diffusion filtering and then by an automatic threshold technique. The lesion is segmented by the level set method in the combined image. The texture, strain, and shape features are computed from the segmented lesions. Some of the features are distinct in an elastogram for

TABLE 6. Performance Analysis of the FIS Classifier

Parameters	Type of Lesion Specified by Radiologist	Total Lesions	Correctly Detected	%
Sensitivity (in detecting malignant solid masses)	Malignant	13	13	100
Specificity (in detecting benign solid masses and benign cysts)	Benign solid mass + benign cyst	27	20	74
Accuracy		40	33	83

the 3 specified conditions, and hence, elastogram increases the specificity of diagnosis.

In the proposed method, the breast lesion is detected and then classified using both ultrasound B-mode imaging and elastogram. The cystic lesions are differentiated from benign solid masses and malignancy. The proposed algorithm gives higher accuracy in detecting malignant and benign solid masses but yields less accuracy in classifying cyst. Cystic lesions have almost the same characteristics as that of benign solid masses. However, in certain cases of simple cysts, we were able to segment the anechoic portion only. Texture, strain, and shape features are extracted from this anechoic portion. However, these features were not representative of simple cysts, which led to an incorrect classification.

If both anechoic and thin echoic portions of the simple cyst are properly segmented out, the accuracy of classification can be improved. In future, this will be done using other segmentation techniques and it can be extended to identify the types of malignancy of lesions.

REFERENCES

- Samani A, Zubovits J, Plewes D. Elastic moduli of normal and pathological human breast tissues: an inversion-technique-based investigation of 169 samples. *Phys Med Biol.* 2007;52:1565–1576.
- Stavros AT, Thickman D, Rapp CL, et al. Solid breast nodules: use of sonography to distinguish between benign and malignant lesions. *Radiology.* 1995;196:123–134.
- Yaffe MJ. Measurement of mammographic density. *Breast Cancer Res.* 2008;10:209.
- Ophir J, Cespedes I, Garra B, et al. Elastography: ultrasonic imaging of tissue strain and elastic modulus in vivo. *Eur J Ultrasound.* 1996;3:49–70.
- Parkin DM, Bray F, Ferlay J, et al. Global cancer statistics. *J Clin.* 2005;55:74–108.
- Ophir J, Alam SK, Garra B, et al. Elastography: ultrasonic estimation and imaging of the elastic properties of tissues. *Proc Instn Mech Engrs.* 1999;213:203–233.
- Rago T, Santini F, Scutari M, et al. Elastography: new developments in ultrasound for predicting malignancy in thyroid nodules. *J Clin Endocrinol Metabolism.* 2007;92:2917–2922.
- Wilson T, Chen Q, Zagzebski JA, et al. Initial clinical experience imaging scatterer size and strain in thyroid nodules. *J Ultrasound Med.* 2006;25:1021–1029.
- Ophir J, Cespedes I, Ponnekanti H, et al. Elastography: a quantitative method for imaging the elasticity of biological tissues. *Ultrasound Imaging.* 1991;13:111–134.
- Ophir J, Alam SK, Garra B, et al. Elastography: Imaging of the elastic properties of soft tissues with ultrasound. *J Med Ultrasonics.* 2002;29:155–171.
- Hall TJ, Zhu Y, Spalding CS. In vivo real-time freehand palpation imaging. *Ultrasound Med Biol.* 2003;29:427–435.
- Konofagou EE, Harrigan T, Ophir J, et al. Shear strain estimation and lesion mobility assessment in elastography. *Ultrasonics.* 2000;38:400–404.
- Barr RG. Real-time ultrasound elasticity of the breast. Initial clinical results. *Ultrasound Quarterly.* 2010;26:61–66.
- Chen E, Ph.D. dissertation, University of Illinois at Urbana-Champaign, 1995.
- Garra BS, Cespedes EI, Ophir J, et al. Elastography of breast lesions: initial clinical results. *Radiology.* 1997;202:79–86.
- Steinberg BD, Sullivan DC, Birbaum JA. Sonographic discrimination between benign and malignant breast lesions with the use of disparity processing. *Acad Radiol.* 2001;8:704–712.
- Moon WK, Chang RF. Solid breast masses: classification with computer-aided analysis of continuous US images obtained with probe compression. *Radiology.* 2005;236:458–464.

18. Liu W, Zagszebski JA, Varghese T, et al. Segmentation of elastographic images using a coarse-to-fine active contour model. *Ultrasound Med Biol.* 2007;32:397–408.
19. Xia R, Liu W, Zhao J, et al. An optimal initialization technique for improving the segmentation performance of Chan-veese model. *IEEE Int Conf Automation Logistics.* 2007;18:411–415.
20. Yongjian Y, Acton ST. Speckle reducing anisotropic diffusion. *IEEE Transact Image Proc.* 2002;11:1260–1270.
21. Li C, Xu C, Gui C, et al. Level set evolution without reinitialization: a new variational formulation. *Proc IEEE Comput Soc Conf Comput Vis Pattern Recognit.* 2005;430–436.
22. Osher S, Sethian JA. Fronts propagating with curvature- dependent speed: algorithms based on Hamilton–Jacobi formulations. *J Comp Phys.* 1988;79:12–49.
23. Otsu N. A threshold selection method from gray-level histograms. *IEEE Trans Systems Man Cybernetics.* 1979;9:62–66.
24. Barr RG, Lackey AE. The utility of the “bull’s-eye” artifact on breast elasticity imaging in reducing breast lesion biopsy rate. *Ultrasound Q.* 2011;27:151–155.
25. Selvan S, Kavitha M, Shenbaga Devi S, et al. Feature extraction for characterization of breast lesions in ultrasound echography and elastography. *J Comp Sci.* 2010;6:67–74.
26. Zunic J, Rosin P. A new convexity measure for polygons. *IEEE Trans Pattern Anal Mach Intell.* 2004;26:923–934.
27. Selvan S, Shenbaga Devi S, Kavitha M, et al. Automatic segmentation and feature extraction of breast lesions. *Int J Comp Intelligence Healthcare Inform.* 2010;3:65–69.
28. Haralick R, Shanmugam K, Dinstein I. Texture features for image classification. *IEEE Transactions on Systems, Man Cybernetics.* 1973;3:610–621.
29. Zhan Q, Molenaar M, Gorte B. Urban land use classes with fuzzy membership and classification based on integration of remote sensing and GIS. *ISPRS.* 2000.